04,14

Acoustic emission in case of impact damage to cement stone, statically compressed orthogonally to the impact

© A.G. Kadomtsev, I.P. Shcherbakov, A.E. Chmel¶

Ioffe Institute,
St. Petersburg, Russia

¶ E-mail: chmel@mail.ioffe.ru

Received October 18, 2024
Revised October 18, 2024
Accepted October 19, 2024

Uniaxially compressed cement stone samples M-400 were subjected to point impact damage during orthogonally directed compression. The impact-induced acoustic emission generation was recorded in the range of 400−600 kHz. The threshold of impact fracture (fragmentation of the sample) without applying a compressive load was preliminarily determined. It was found that the energy distributions in the time sweeps of acoustic emission without compression of the sample followed a power law characteristic of the process of cooperative microcrack formation. The energy distributions in acoustic emission pulses under constant compressive load showed an exponential function typical of random, non-interacting sources of acoustic emission that occur with an increase of the density of cement stone. When compression was close to the ultimate tensile strength of the material, the impact caused a „pre-threshold" macroscopic destruction of the samples (trigger effect).

Keywords: cement stone, static load, impact fracture, trigger effect, acoustic emission.

DOI: 10.61011/PSS.2024.11.60086.267

1. Introduction

The acoustic emission (AE) method is one of the basic methods for detecting stable structural defects and monitoring the accumulation of microscopic damage in various heterogeneous materials — primarily concretes [1–3] and rocks [4–6], experiencing both static and dynamic loads. The AE analysis of building materials pays much attention to non-destructive testing of the condition of facilities [7,8] (identification of stable or slowly progressing voids, cracks and extraneous inclusions), whereas the acoustic emission studies in the experimental seismology mainly focus on the analysis of active fracture processes. Nevertheless, papers have appeared in the last decade that study the dynamic properties of compressed cement stone (CS) using laboratory methods derived from the rock testing experience [9–14]. This particular application was implemented during the present work for the analysis of acoustic signals from CS samples, to which a complex mechanical load was applied.

The samples were subjected to orthogonally directed impacts of a pointed striker under a variable static compressive load, which created local damage on the lateral surface of the object. This loading geometry was chosen as close to the actual distribution of mechanical impact in construction structures, the lower elements of which are compressed vertically, and propagating seismic waves, tides, waves of volcanic activity etc. act on the lateral surfaces.

2. Samples and equipment

Plates made of a cement stone naturally hardened for 28 days were used in this study; the size of the plates is $10 \times 10 \times 40$ mm. Photo of the setup for sample loading is shown in Figure 1. Compressive pressure was applied along the largest plate size. The impact wave in a uniaxially compressed sample was excited by the orthogonally static load. Sample surface damage was induced by a pointed die attached to a pendulum. A support plate was placed behind the sample to avoid its horizontal displacement during impact.

Die energy was constant and equal to 0.1 J. Ultimate (threshold) compression load (without impact load) P_{ul} was preliminary measured. The current load P was varied stepwise from 0 to a critical value at which global destruction of the sample occurred upon impact. AE time scans were recorded after each impact by a wide-band piezoelectric transducer made of high-sensitivity PZT ceramics which was attached to the side surface of the sample. Acoustic emission generation was recorded in the range of 400−600 kHz for 3 ms with a time resolution of 40 ns.

3. Results and discussion

3.1. Impact at $P = 0$

Figure 2, *a* shows the AE signal sweep upon impact on a sample without applying static voltage. The intensity (square of the signal amplitude, A^2) of AE is proportional to the energy E released in case of the formation of a point damage: $E \propto A^2$.

Figure 2, *b* in double logarithmic coordinates shows the energy distribution in the pulse series shown in Figure 2, *a*. The distribution is given in the form of a dependence $N(E > \varepsilon)$ versus ε, in which the ordinate contains the

Figure 1. Photo of a setup for generating AE in case of impact damage to a uniaxially compressed sample CS.

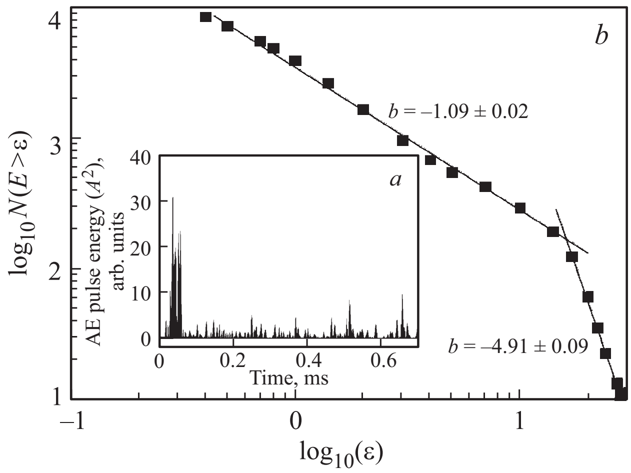

Figure 2. The time scale of the amplitudes squared after impact on the sample at $P = 0$ (a) and the energy distribution in time series A^2 upon impact (b).

number of pulses N, the energy E of which exceeds the „threshold" ε shown on the abscissa, on which the values of the pulse energy are plotted. It can be seen that the energy distributions have log-linear sections corresponding to the Gutenberg-Richter type relationship:

$$\log_{10} N(E > \varepsilon) \propto -b \log_{10} \varepsilon \tag{1}$$

or in the power form:

$$N(E > \varepsilon) \propto \varepsilon^{-b}. \tag{1a}$$

The parameter b in (1) defines the slope of straight segments. The lower the value of b, the greater is the quantity of high-energy AE pulses during the degradation of the material. The „kink" of the log-linear dependence indicates the presence of two scales of accumulation of local weaknesses in the structure of the CS.

The variation of this parameter was considered in Ref. [11] (within the framework of the accepted ideology of seismic dynamics) as an indicator of the process of structural restructuring during the destruction of loaded concrete blocks. The estimation of the parameter b [12] was used to predict dangerous conditions of facilities in a similar approach to the problem of diagnostics of concrete elements of structures.

3.2. Impact at $P_{ul} > 0$

The sweep of the emission of the application of the static load $P = 0.3P_{ul}$ in case of impact on the sample is shown in Figure 3. The energy distribution in the pulses of induced AE (Figure 4) has changed significantly. The energy distribution in this series of pulses is plotted in Figure 4, a in double logarithmic coordinates. A log-linear relationship is not observed in contrast to the distribution calculated for a sample without static load (Figure 2, b). However, the graph of dependence $\log_{10} N(E > E')$ on E' in semi-logarithmic coordinates (with linear scale along the energy axis) lies on straight lines corresponding to the ratio:

$$\log_{10} N(E > \varepsilon) \propto -a\varepsilon \tag{2}$$

Or, what too:

$$N(E > \varepsilon) \propto \exp(-a\varepsilon), \tag{2a}$$

where a is a constant (slope of a straight line on the graph). The exponential ratio of the Poisson type (2a) indicates the random nature of the occurrence of AE sources.

The transition from correlated to random accumulation of microcracks can be explained by the high porosity of cement M-400 (about 30%). It is well known that its porosity

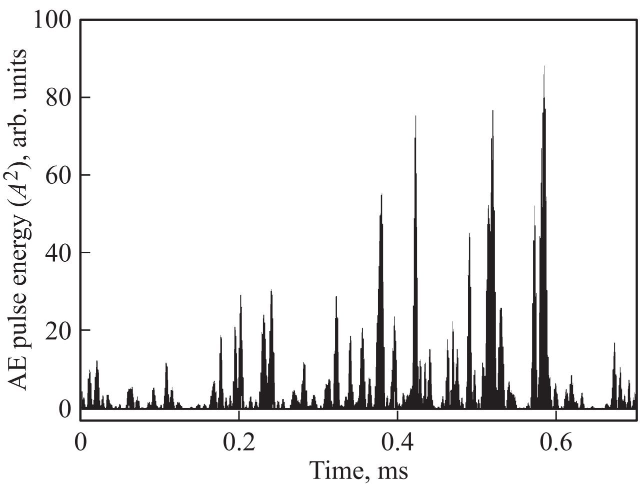

Figure 3. Time sweep of amplitudes A^2 after impact on a sample under pressure $P = 0.3P_{ul}$.

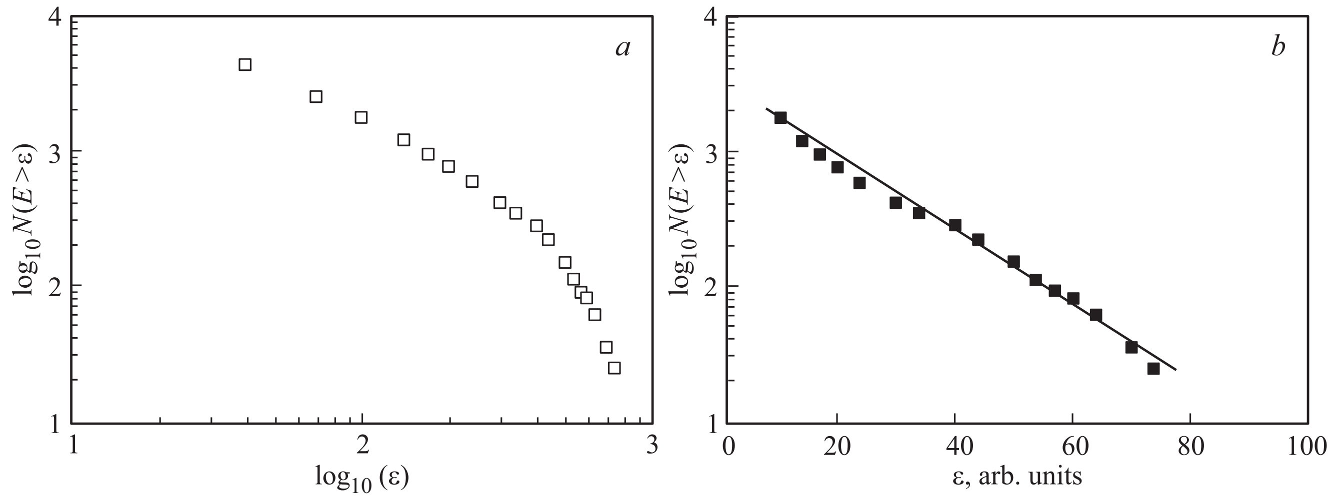

Figure 4. Energy distribution in time series of AE in case of an impact on a sample under static load $P = 0.3P_{ul}$, plotted in double logarithmic (a) and semi-logarithmic (b) scales.

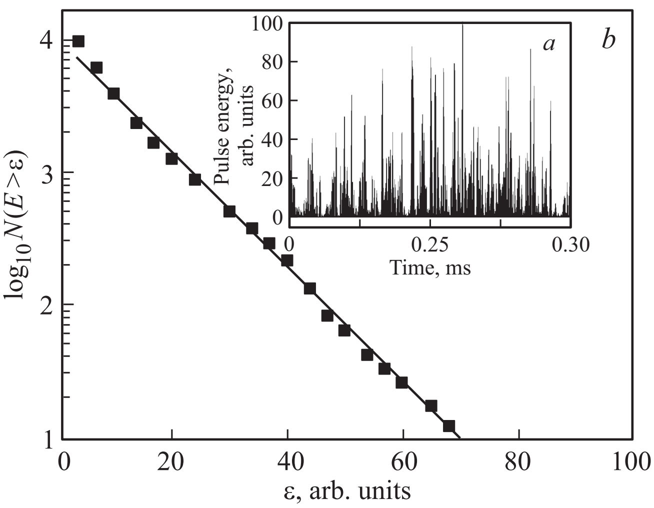

Figure 5. Time sweep of AE amplitudes after impact on the sample (a) and energy distribution of acoustic pulses (b) at $P = 0.6P_{ul}$.

significantly decreases even with a slight compression of the CS, which leads to a decrease of the „reservoir of weak points" in the material [15]. Accordingly, the radius of the required interaction increases, that is, the size of the newly formed crack becomes less than the distance to the nearest weak point.

When the compressive pressure increases to $P = 0.6P_{ul}$, the intensity of AE slightly increases compared to the load $P = 0.3P_{ul}$ (cf. Figure 3 and Figure 5, a), and the energy distribution also follows an exponential law (Figure 5, b). At the same time, the slope of the straight line in the last graph (the value of the parameter a) is higher than in the graph in Figure 5, a, which indicates a smaller contribution to the energy distribution from large microcracks.

The next compressive pressure was close to the threshold of destruction of free samples: $P = 0.9P_{ul}$. In this case, the pulse intensity in the AE sweep turned out to be almost an order of magnitude higher than in the three previous static loading modes.

In addition, the series of pulses were concentrated in two or three separated peaks (Figure 6, a), with the last peak preceding the „pre-threshold" ($P < P_{ul}$) destruction — trigger failure.

The distribution of energy in AE pulses (Figure 6, b) returned to correlated accumulation according to the Gutenberg-Richter law type. The impact load under conditions of compressive pressure close to the threshold of fracture induces not a dispersed accumulation of microcracks but a sequential formation of several strong fracture nuclei in which effective interaction of microcracks took

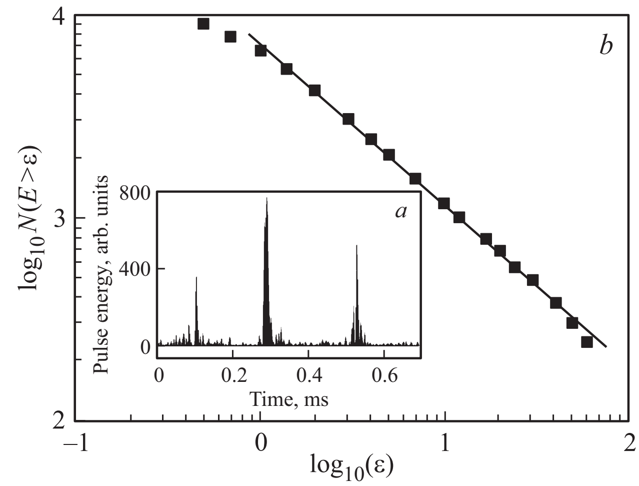

Figure 6. Temporal sweep of AE amplitudes after impact on the sample (a) and energy distribution of acoustic pulses (b) at $P = 0.9P_{ul}$.

place. Therefore, the first AE overshoots at $P = 0.9P_{ul}$, (Figure $6, a$) after which the sample retained shape stability, play the role of a „pre-trigger".

4. Conclusion

The statistics of microcrack accumulation in a single-compressed cement stone under orthogonal impact load is considered. The problem is relevant for the safety of concrete foundations of structures experiencing lateral mechanical impulse effects of natural and man-made origin. The formation of microcracks in case of a side impact was recorded by the AE method. Statistical processing of the time series of AE pulses made it possible to differentiate either the random (dispersed) or correlated (interaction-related) nature of microdamage accumulation. The CS M-400 used in the experiments has a high porosity (28%). Therefore, the impact damage to multiple partitions between pores in statically unloaded samples causes a long-range effect of collective accumulation of microcracks according to a power law. The application of a uniaxial static load significantly increases the density of the material, which leads to an isolated accumulation of non-interacting microcracks according to an exponential law.

Finally, large fracture nuclei appear in the mass of the material at a static load close to the CS destruction threshold in which the interaction between microcracks occurs again leading to a trigger failure.

Conflict of interest

The authors declare the absence of conflicts of interest.

References

[1] D.G. Aggelis. Mech. Res. Commun. **38**, 153 (2013).
[2] D.D. Mandal, M. Bentahar, A. El Mahi, A. Brouste, R. El Guerjouma, S. Montresor, F.B. Cartiaux. Materials. **15**, 3486 (2022).
[3] A. Carpinteri, J. Xu, G. Lacidogna, A. Manuello. Cem. Concr. Compos. **34**, 529 (2012).
[4] J. Davidsen, T. Goebel, G. Kwiatek, S. Stanchits, J. Baró, G.J. Dresen. Geophys Res: Solid Earth. **126**, e2021JB022539 (2021).
[5] B. Haimson, C. Chang. Int. J. Rock. Mech. Min. **37**, 285 (2000).
[6] V.B. Smirnov, A.V. Ponomarev, A.D. Zavyalov. Izvestiya. Phys. Solid Earth. **31**, 38 1995.
[7] M. Brigante, M.A. Sumbatyan. Defektoskopiya **4**, 3 (2013). (in Russian).
[8] A.I. Sagaidak. Vestnik NIC „Stroitel'stvo". **38**, 63 (2023). (in Russian).
[9] I. Dakanali, A. Kyriazopoulos, I. Stavrakas, D. Triantis. Proc. Intern. Conference: Science in Technology 2015 Athens, Greece.
[10] I.S. Colombo, I.G. Main, J. Mater. Civ. Eng. **15**, 280 (2003).
[11] C. Guzmána, D. Torresa, C. Hucailuka, D. Filipussi. Proc. Mater. Sci. **8**, 148 (2015).
[12] R. Vidya Sagar, B.K. Raghu Prasad, R.K. Singh. In book: Acoustic emission (AE) and related Non-destructive evaluation (NDE) techniques in fracture mechanics of concrete Ed.: M. Ohtsu, Woodhead publishing, 2015.
[13] J.X. Zhengwu, F. Qinghua, H.G. Lacidogna, A. Carpinteri. Struct. Health Monit. **17**, 147592171773053 (2017).
[14] A. Esmaeilzadeh, M. Nikkhah, E. Eidivandi. Geopersia. **13**, 49 (2023).
[15] V.I. Betekhtin, A.N. Bakhtibayev, A.G. Kadomtsev, D.A. Imanbekov. Tsement, **5–6**, 16 (1991). (in Russian).

Translated by A.Akhtyamov